



iJRASET

International Journal For Research in
Applied Science and Engineering Technology



INTERNATIONAL JOURNAL FOR RESEARCH

IN APPLIED SCIENCE & ENGINEERING TECHNOLOGY

Volume: 5 Issue: VIII Month of publication: August 2017

DOI: <http://doi.org/10.22214/ijraset.2017.8269>

www.ijraset.com

Call: ☎ 08813907089

E-mail ID: ijraset@gmail.com

A Novel Hybrid Fuzzy Controller for Grid Connected DFIG Wind System

Andra Sridevi¹, Y. Vishnu Murthulu²

¹M.Tech Student Scholar, ²M.Tech, Assistant Professor, Department of Electrical & Electronics Engineering, PVP Siddhartha Engineering College, Kanuru, Vijayawada, Krishna (Dt), AP, India.

Abstract: In this project Hybrid Fuzzy controller for grid connected DFIG wind system is presented. Doubly-fed induction generators (DFIG) are more increasingly used for the large wind power generation. The proposed control algorithm is applied to a doubly fed induction generator (DFIG) whose stator is directly connected to the grid and the rotor is connected to the grid through a back-to-back AC-DC-AC PWM converters. Fuzzy control has been widely applied to power electronics system; Fuzzy control is applied to control DFIG. Another PI regulator is used to control the grid side converter (GSC) by using the oriented voltage control strategy. The control of the rotor-side converter is realized by stator flux oriented control and the fuzzy controller performs robust speed control. The grid side converter (GSC) is controlled in such a way to guarantee a smooth DC voltage and ensure sinusoidal current in the grid side. The system performance can be observed by using MATLAB/SIMULINK software. In extension Hybrid Fuzzy based grid connected DFIG wind system is used for better speed control performance.

Keywords: DFIG, Fuzzy Controller, Hybrid Fuzzy Controller, Wind Energy Conversion System.

I. INTRODUCTION

More and more dc loads such as light-emitting diode (LED) lights and electric vehicles (EVs) are connected to ac power systems to save energy and reduce CO₂ emission. When power can be fully supplied by local renewable power sources, long distance high voltage transmission is no longer necessary. Hybrid AC/DC micro grids [1] have been proposed to facilitate the connection of renewable power sources to conventional ac systems. However, dc power from the renewable photovoltaic (PV) panels or fuel cells has to be converted into ac using dc/dc boosters and dc/ac inverters in order to connect to an ac grid. In an ac grid, embedded ac/dc and dc/dc converters are required for various home and office facilities to supply different dc voltages.

Layers control there is a high- With increase in contribution of wind power into electric power grid, energy storage devices will be required to dynamically match the intermitting of wind energy. When wind turbines are connected to a grid, they should always maintain constant power. In order to maintain constant active power, the use of Doubly-Fed Induction Generators (DFIG) with Energy Storage System (ESS) like super capacitor (or) batteries can be used, with a two layer control scheme. In the two layer controller known as Wind Farm Supervisory Control (WFSC), which generates the active power (P), Stator Power (P_s), Energy storage power (P_e), DC voltage (V_{dc}) etc., references for the low layer WTG controllers. The low-layer controller has two different controls i.e., Grid side controller (GSC) and Rotor side controller (RSC) which are used to control the AC/DC/AC converters of DFIG wind turbines and to generate the desired active power demand specified by the grid operator.

With increased penetration of wind power into electrical grids, Doubly-Fed Induction Generator (DFIG) wind turbines are largely deployed due to their variable speed feature and hence influencing system dynamics. This has created an interest in developing suitable models for DFIG to be integrated into power system studies. The continuous trend of having high penetration of wind power, in recent years, has made it necessary to introduce new practices. Additionally, in order to model power electronic converters, in the simplest scenario, it is assumed that the converters are ideal and the DC-link voltage between the converters is constant. Consequently, depending on the converter control, a controllable voltage (current) source can be implemented to represent the operation of the rotor-side of the converter in the model. A Fuzzy Logic Controller (FLC) does not require the system model and it can be used as a nonlinear controller. In this project the comparison of various controllers like pi, fuzzy and hybrid fuzzy (PI and Fuzzy) controllers are used to get better speed response which is implemented and verified by using MATLAB/SIMULINK software.

II. SYSTEM CONFIGURATION AND CONTROL PRINCIPLE

The schematic diagram of proposed grid interfaced DFIG based WECS is shown in Fig.1. BESS is connected in the DC link of two back to back connected VSCs. Here the stator is directly connected to the grid. RSC is controlled in voltage oriented reference frame. The d-axis of the synchronously rotating reference frame is oriented along voltage axis using EPLL (Enhanced Phase Locked

Loop). Here, the rotor position computation algorithm is used for the position estimation. GSC is controlled in such a way that the regulated power is fed to the grid. When the power produced is more than the regulated power, and then the remaining power is stored in the BESS. If power produced is less than regulated power, then the BESS supplies the remaining power to the grid. The control algorithms are presented in Fig.2.

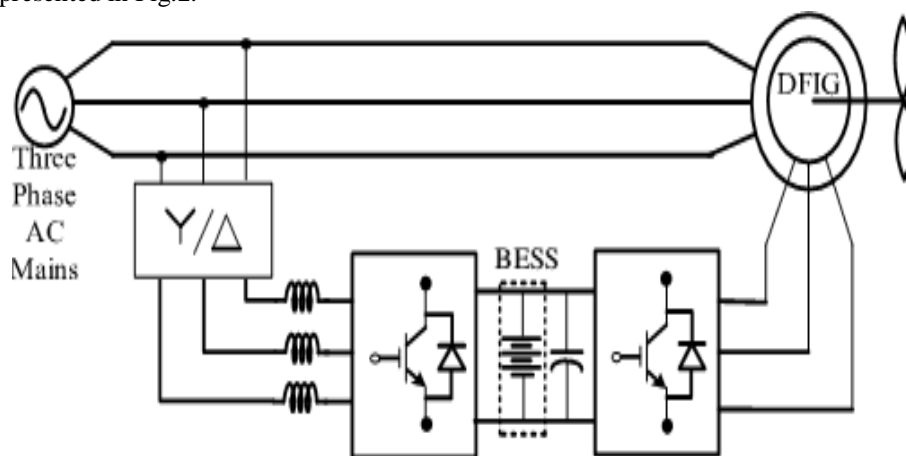


Fig.1. Proposed System Configuration

III. DESIGN OF VARIABLE SPEED WECS

Selection of ratings of converters, BESS voltage and BESS rating are very much important for the successful operation of the WECS. If the battery rating is very high, then the system is reliable but the cost is very high. So the selection of rating of BESS is very critical from economical point of view.

A. Selection of Battery Voltage

In general, DC link voltage of VSC must be greater than twice the peak of phase voltage. The battery voltage is selected by considering voltages at both GSC and RSC. Normally DFIG operating speed range for WECS is between 0.7 p. u. to 1.3 p. u. So the maximum operating slip (S_{max}) is 0.3. The possible maximum RMS phase voltage of the rotor (v_r) is given as,

$$v_r = S_{max} v_p \left(\frac{N_r}{N_s} \right) \quad (1)$$

Where, v_p is the stator phase voltage = 230 V, $S_{max} = 0.3$, N_r/N_s = rotor to stator turns ratio=1, By placing the above values, rotor phase voltage (v_r) is obtained as 34.64 V. There is a star delta transformer between GSC and grid with 2:1 turn's ratio. So, the phase voltage at GSC (V_{GSC}) = 66.67 V. As v_{GSC} is more than v_r , the DC link voltage should be selected according to v_{GSC} . The DC link voltage is estimated as,

$$V_{dc} \geq (\sqrt{2}/m) v_{GSC} \quad (2)$$

Maximum modulation index of VSC is selected as 1 for linear region. So the value of V_{dc} by (2) is 188.57 V. By considering the battery voltage for the minimum state of charge (SOC), and also considering the availability of the battery in the system, the nominal battery voltage is selected as 240 V.

B. Design of Battery Energy Storage System (BESS)

Large size of the battery increases the reliability but also increases the initial investment. However, small rating of the battery affects the reliability. So the proper design of BESS is necessary for the satisfactory operation of the proposed WECS. The storage capacity of the BESS depends upon the approximate wind profile at the site. The rating of the BESS is decided by the total energy stored in to the battery. In this proposed DFIG, the constant value of the power feeding to the grid is selected as the average value of the power generation from the previous wind data. So the energy stored in to the BESS, when the power generated from the DFIG is more than the regulated power. On the other hand, the energy is taken from the BESS, when the power generation is less than the regulated power. The average power is selected from a past wind data of a particular wind site. In this work, the wind speed of is taken from the calculation of average power. The wind data is given at 20 meters height in the website for every one hour throughout the day. However, practically the turbine is installed at much higher height. The wind speed at turbine height is calculated as,

$$\frac{v}{v_0} = \left(\frac{h}{h_0}\right)^n \quad (3)$$

Where, v is the new wind speed at a height h , v_0 is the old wind speed at a height of h_0 and n is terrain factor. Here in this work, a terrain factor of 0.13 is selected for the wind speed calibration. So the wind speeds are calculated at 50m height and the power outputs of the DFIG at that wind speeds. The average power (P_{avg}) generated for a day. This average power may be calculated by considering every day or a month. The rating of the battery bank is calculated as,

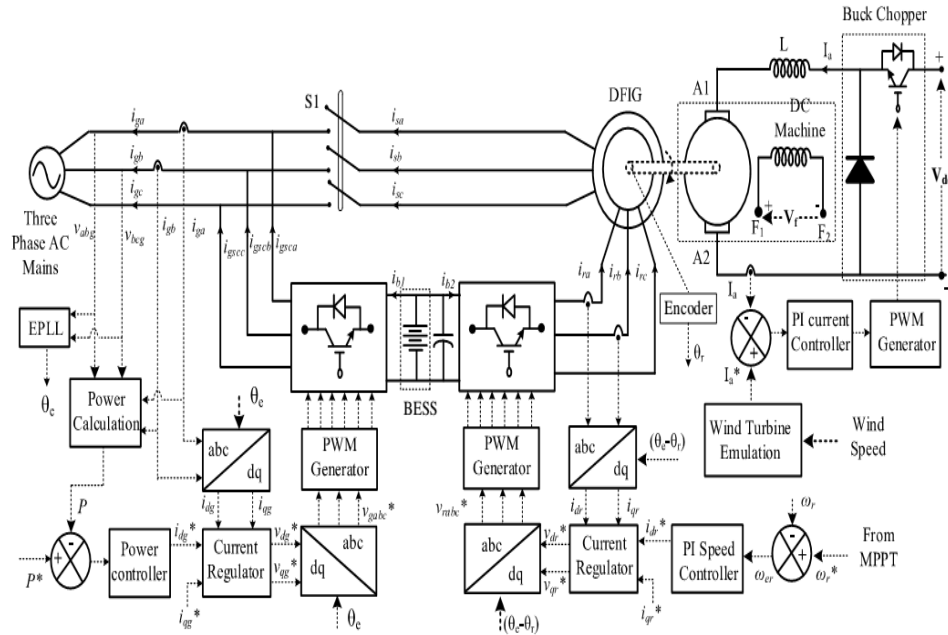


Fig.2. Control Algorithm of the proposed WECS

$$E_b = \sum_{i=1}^n (P_{mi} * t_i) \quad (4)$$

Where, P_{mi} is the excess power stored into the battery at every instant and t_i is the time period taken as 5 minutes in this case. P_{mi} is calculated as,

$$P_{mi} = P_{inst} - P_{avg} \quad (5)$$

Where P_{inst} is the instantaneous power at any instant and P_{avg} is the average power fed to the grid.

C. Selection of Voltage Source Converters (VSC) Rating

The power flows through RSC and GSC are different because of BESS in the DC link. The maximum power flows through the GSC, when the wind turbine is in shut down condition and the BESS is feeding the whole power to the grid. This constant power generation is normally selected as average power which is 3.85 kW in this case. Therefore, the GSC rating is selected as 3.85kVA. RSC rating depends upon the reactive power supplied from the rotor side for realizing unity power factor at the stator side and also the rotor active power. The DFIG draws a lagging volt-ampere reactive (VAR) for its excitation to build the rated air gap voltage. It is calculated from the machine parameters that the lagging VAR of 2 kVAR is needed when it is running as a motor. In DFIG case, the operating speed range is 0.7 p.u. to 1.3 p.u. So the maximum slip (s_{max}) is 0.3. For achieving unity power factor at the stator side, reactive power of 600 VAR ($s_{max} * Q_s = 0.3 * 2 \text{ kVAR}$) is needed from the rotor side (Q_{rmax}). Maximum rotor active power is $s_{max} * P$. The power rating of the DFIG is 5 kW. Therefore, the maximum rotor active power (P_{rmax}) is 1.5kW ($0.3 * 5 \text{ kW} = 1.5 \text{ kW}$). So the rating of the VSC used as RSC, S_{rated} is estimated as,

$$S_{rated} = \sqrt{P_{rmax}^2 + Q_{rmax}^2} \quad (6)$$

Thus kVA rating of RSC, S_{rated} is calculated as 1.615 kVA.

IV. CONTROL STRATEGY

Control algorithms of GSC, RSC and sensor less operation of DFIG are discussed. A schematic diagram of control for GSC and RSC are presented in Fig.2.

A. Control of RSC

An independent control of both active and reactive powers is achieved by the RSC. Through this RSC control, the maximum power point is achieved operationally. RSC is controlled in voltage oriented reference frame. So the active and reactive powers are controlled by controlling d and q axis rotor reference currents (I_{dr} and I_{qr}), respectively. Direct axis rotor reference current (I_{dr}^*) is obtained through PI (Proportional Integral) speed controller by processing the speed error (ω_{er}) between reference and estimated rotor speeds (ω_r^* and ω_r) as,

$$I_{dr}^*(n) = I_{dr}^*(n-1) + K_{pd}[\omega_{er}(n) - \omega_{er}(n-1)] + K_{id} \omega_{er}(n) \quad (7)$$

Where, k_{pd} , k_{id} are the proportional and integral gains of speed controller. $\omega_r(n)$ and $\omega_r(n-1)$ are the speed errors at n th and $(n-1)$ th instant. $I_{dr}^*(n)$ and $I_{dr}^*(n-1)$ are the direct axis rotor reference currents at n th and $(n-1)$ th instant. Reference speed (ω_r^*) is selected for achieving MPPT. In this algorithm, the reference rotor speed is estimated using tip speed ratio (TSR) control using wind speed. The reference quadrature axis rotor current (I_{qr}^*) is selected to control the reactive power to zero at stator terminals. The direct and quadrature axis rotor currents (I_{dr} and I_{qr}) are computed from sensed rotor currents (i_{ra} , i_{rb} and i_{rc}) as,

$$I_{dr} = \frac{2}{3} \left[i_{ra} \sin \theta_{slip} + i_{rb} \sin \left(\theta_{slip} - \frac{2\pi}{3} \right) + i_{rc} \sin \left(\theta_{slip} + \frac{2\pi}{3} \right) \right] \quad (8)$$

$$I_{qr} = \frac{2}{3} \left[i_{ra} \cos \theta_{slip} + i_{rb} \cos \left(\theta_{slip} - \frac{2\pi}{3} \right) + i_{rc} \cos \left(\theta_{slip} + \frac{2\pi}{3} \right) \right] \quad (9)$$

Where, slip angle (θ_{slip}) is calculated as,

$$\theta_{slin} = \theta_e - \theta_r \quad (10)$$

The voltage angle θ_e is calculated using EPLL (Enhanced Phase Locked Loop) as shown in Fig.3. The rotor position (θ_r) is calculated using RPCA sensor less algorithm.

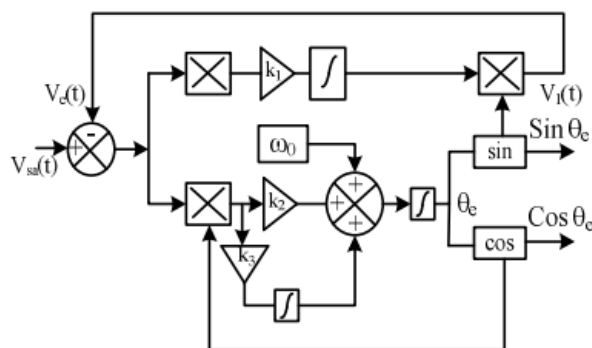


Fig.3. Enhanced Phase Locked Loop (EPLL)

The direct and quadrature axis rotor currents (I_{dr} and I_{qr}) are controlled close to reference direct and quadrature axis rotor currents (I_{dr}^* and I_{qr}^*) by using two current controllers. The direct and quadrature rotor current errors (I_{dr} , I_{qr}) between estimated (I_{dr} , I_{qr}) and reference (I_{dr}^* , I_{qr}^*) direct, quadrature axis rotor currents are processed through PI controllers for achieving reference direct and quadrature axis rotor voltages (V_{dr}' and V_{qr}') as,

$$V_{dr}(n) = V_{dr}(n-1) + K_{pdr}\{I_{der}^*(n) - I_{der}^*(n-1)\} + K_{idr}I_{der}^*(n) \quad (11)$$

$$V_{gr}(n) = V_{gr}(n-1) + K_{gav}\{I_{ger}^*(n) - I_{ger}^*(n-1)\} + K_{iav}I_{ger}^*(n) \quad (12)$$

Where k_{pdr} , k_{idr} are the proportional and integral gains of direct axis current controller, k_{pqv} , k_{iqv} are the proportional and integral gains of quadrature axis current controller. $I_{dr}(n)$ and $I_{dr}(n-1)$ are the direct axis current errors at nth and (n-1)th instant. $V_{dr}'(n)$ and $V_{dr}'(n-1)$ are direct axis rotor voltages at nth and (n-1)th instant. $I_{qr}(n)$ and $I_{qr}(n-1)$ are the quadrature axis rotor current errors at nth and (n-1)th instant. $V_{qr}'(n)$ and $V_{qr}'(n-1)$ are quadrature axis rotor voltages at nth and (n-1)th instant. Direct and quadrature axis rotor voltages (V_{dr}' and V_{qr}') are added with the compensation terms for achieving reference rotor voltages (V_{dr}^* and V_{qr}^*) as,

$$V_{dr}^* = V_{dr} - (\omega_e - \omega_r) \sigma L_r I_{qr} \quad (13)$$

$$V_{qr}^* = V_{qr} - (\omega_e - \omega_r) (L_m i_{ms} + \sigma L_r I_{dr}) \quad (14)$$

These reference direct and quadrature voltages (V_{dr}^* , V_{qr}^*) are converted into three phase reference rotor voltages (v_{ra}^* , v_{rb}^* , v_{rc}^*) as,

$$v_{ra}^* = V_{dr}^* \sin \theta_{slip} + V_{qr}^* \cos \theta_{slip} \quad (15)$$

$$v_{rb}^* = V_{dr}^* \sin(\theta_{slip} - \frac{2\pi}{3}) + V_{qr}^* \cos(\theta_{slip} - \frac{2\pi}{3}) \quad (16)$$

$$v_{rc}^* = V_{dr}^* \sin(\theta_{slip} + \frac{2\pi}{3}) + V_{qr}^* \cos(\theta_{slip} + \frac{2\pi}{3}) \quad (17)$$

These three phase rotor reference voltages (v_{ra}^* , v_{rb}^* , v_{rc}^*) are compared with triangular carrier wave of switching frequency for generating the PWM signals for the Insulated Gate Bipolar Transistors (IGBTs) of the RSC.

B. Control of GSC

The novelty of this work lies in the control of GSC. The control of this GSC is realized on voltage oriented reference frame. The active and reactive powers (P & Q) fed to the grid are controlled by controlling direct and quadrature grid currents (I_{dg} & I_{qg}) respectively. Direct axis grid current (I_{dg}) is obtained from the reference power (P^*) as,

$$I_{dg}^* = \left(\frac{2}{3}\right) \left(\frac{P^*}{v_{dg}}\right) \quad (18)$$

For realizing unity power factor at ac mains, I_{qg}^* is selected as zero. Actual direct and quadrature grid currents (I_{dg} and I_{qg}) are estimated from the sensed grid currents. The error (I_{deg} and I_{qeg}) between actual (I_{dg} and I_{qg}) and reference (I_{dg}^* and I_{qg}^*) direct and quadrature currents are processed through a PI controller as shown as

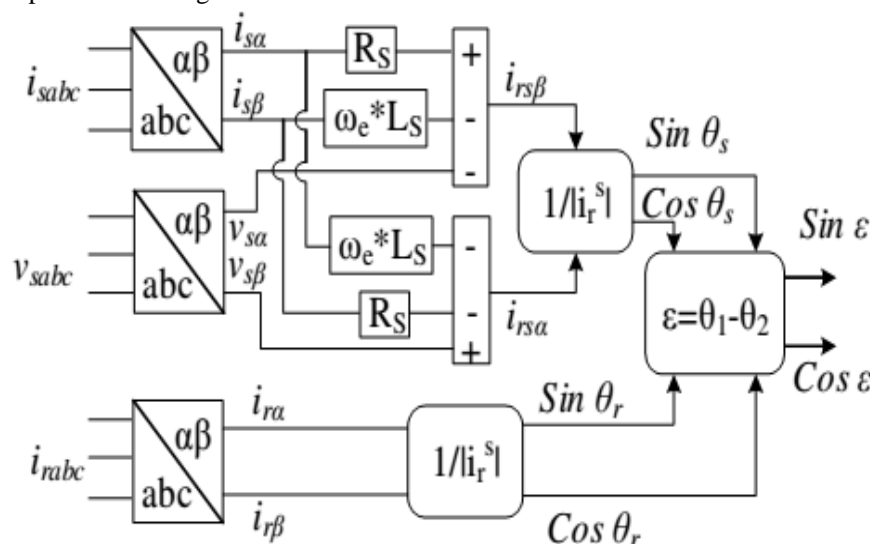


Fig.4. Rotor Position Computation Algorithm

V. CONTROLLERS

A. PI Controller

The proportional plus integral (PI) controller is widely used for industrial applications. The input to the PI controller is the speed error (E), while the output of the PI controller is used as the input of reference current block.

B. Fuzzy Logic Controller

Fuzzy logic control (FLC) is a rule based controller. It is a control algorithm based on a linguistic control strategy which tries to account the human's knowledge about how to control a system without requiring a mathematical model. The approach of the basic structure of the fuzzy logic controller system is illustrated in Fig.5.

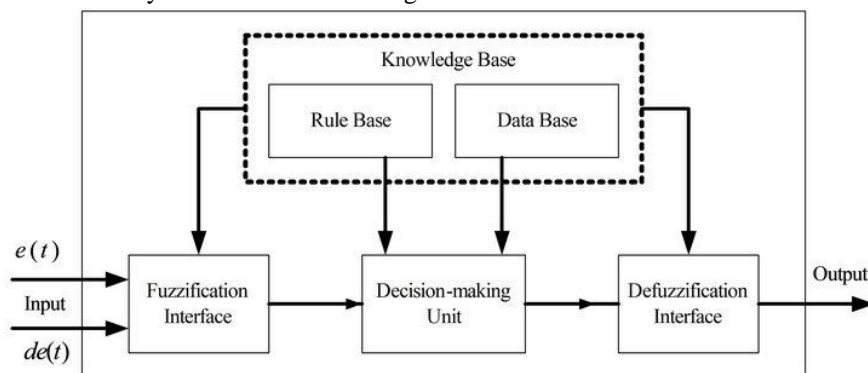


Fig.5 Basic structure of Fuzzy Logic controller

Fuzzy logic uses linguistic variables instead of numerical variables. The process of converting a numerical variable (real number or crisp variables) into a linguistic variable (fuzzy number) is called Fuzzification. Here the inputs for Fuzzy Logic controller are the speed error (E) and change in speed error (CE). Speed error is calculated with comparison between reference speed and the actual speed. The fuzzy logic controller is used to produce an adaptive control so that the motor speed can accurately track the reference speed. The reverse of Fuzzification is called Defuzzification. The use of Fuzzy Logic Controller (FLC) produces required output in a linguistic variable (fuzzy number). According to real world requirements, the linguistic variables have to be transformed to crisp output. The membership function is a graphical representation of the magnitude of participation of each input.

There are different memberships functions associated with each input and output response. Here the trapezoidal membership functions are used for input and output variables. The number of membership functions determines the quality of control which can be achieved using fuzzy controller. As the number of membership function increases, the quality of control improves. As the number of linguistic variables increases, the computational time and required memory increases. Therefore, a compromise between the quality of control and computational time is needed to choose the number of linguistic variables. The most common shape of membership functions is triangular, although trapezoidal and bell curves are also used, but the shape is generally less important than the numbers of curves are also used, but the shape is generally less important than the number of curves and their placement.

The processing stage is based on a collection of logic rules in the form of IF-THEN statements, where the IF part is called the "antecedent" and the THEN part is called the "consequent". The knowledge base comprises knowledge of the application domain and the attendant control goals. It consists of a data "base" and a linguistic (fuzzy) control rule base. The data base provides necessary definitions, which are used to define linguistic control rules and fuzzy data manipulation in an FLC. The rule base characterizes the control goals and control policy of the domain experts by means of a set of linguistic control rules. Decision making logic is the kernel of an FLC. The most important things in fuzzy logic control system designs are the process design of membership functions for input, outputs and the process design of fuzzy if-then rule knowledge base. Fig.6 shows the membership function of speed error (E), change in speed error (CE) and figue.7 shows the membership function of output variable. In practice, one or two types of membership functions are enough to solve most of the problems. The next step is to define the control rules. There are no specific methods to design the fuzzy logic rules. However, the results from PI controller give an opportunity and guidance for rule justification. Therefore after thorough series of analysis, the total 49 rules have been justified as shown in Table 1.

Table.1 Rule base of Fuzzy logic controller

$\Delta e \backslash e$	NL	NM	NS	EZ	PS	PM	PL
NL	NL	NL	NL	NL	NM	NS	EZ
NM	NL	NL	NL	NM	NS	EZ	PS
NS	NL	NL	NM	NS	EZ	PS	PM
EZ	NL	NM	NS	EZ	PS	PM	PL
PS	NM	NS	EZ	PS	PM	PL	PL
PM	NS	EZ	PS	PM	PL	PL	PL
PL	NL	NM	NS	EZ	PS	PM	PL

The membership function is divided into seven sets: NB: Negative Big, NM: Negative Medium, NS: Negative Small, Z: Zero, PS: Positive Small, PM: Positive Medium, PB: Positive Big.

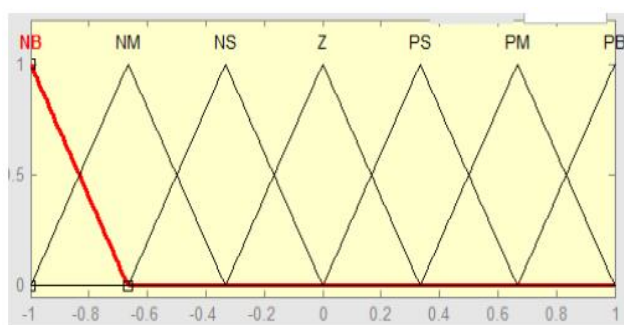


Fig.6. Membership function plots, error and change in error

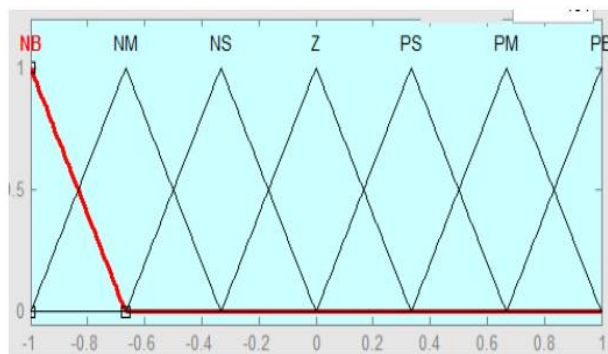


Fig.7. Membership function plots, output variable

C. Hybrid PI-Fuzzy Controller

The objective of the hybrid controller is to utilize the best attributes of the PI and fuzzy logic controllers to provide a controller which will produce better response than either the PI or the fuzzy controller. There are two major differences between the tracking ability of the conventional PI controller and the fuzzy logic controller. Both the PI and fuzzy controller produce reasonably good tracking for steady-state or slowly varying operating conditions. However, when there is a step change in any of the operating conditions, such as may occur in the set point or load, the PI controller tends to exhibit some overshoot or oscillations. The fuzzy controller reduces both the overshoot and extent of oscillations under the same operating conditions. Although the fuzzy controller has a slower response by itself, it reduces both the overshoot and extent of oscillations under the same operating conditions. The desire is that, by combining the two controllers, one can get the quick response of the PI controller while eliminating the overshoot possibly associated with it.

VI. MATLAB/SIMULINK RESULTS

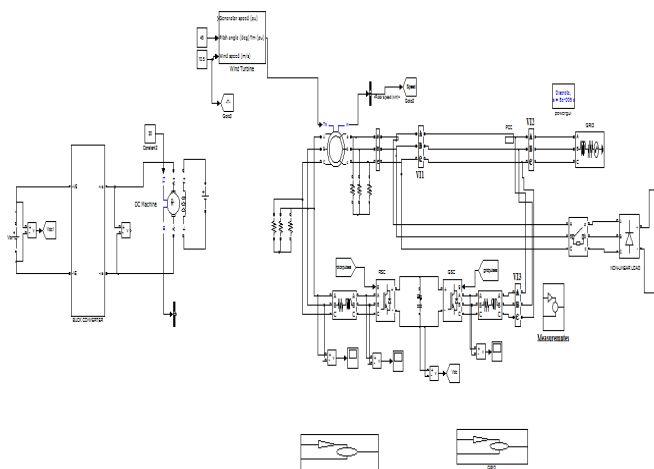
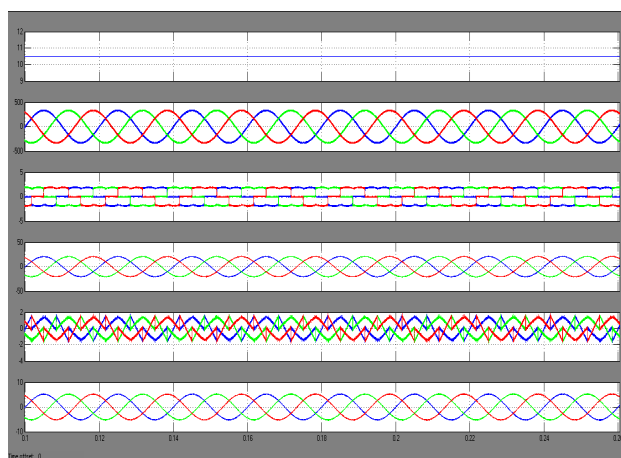
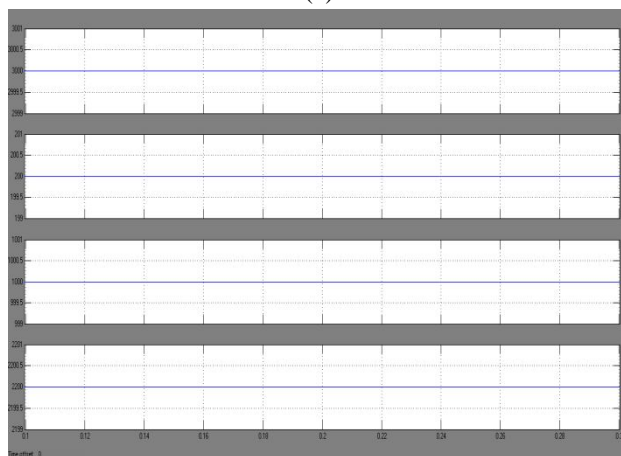


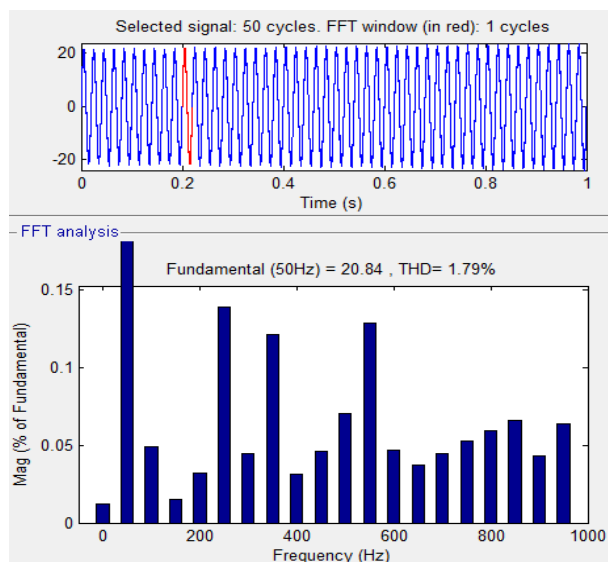
Fig.8. Matlab/Simulink circuit for Control Algorithm of the proposed WECS.



(a)

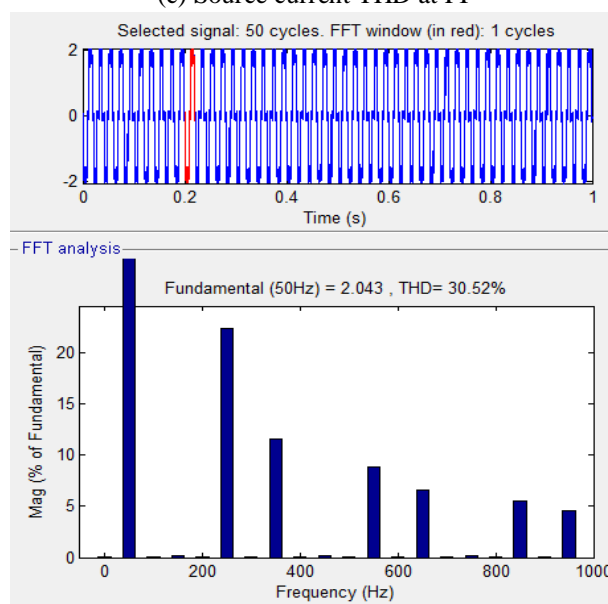


(b) Active and Reactive power components of DFIG



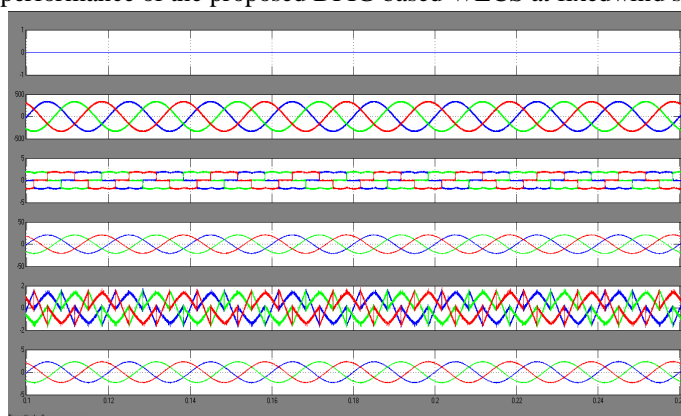
9c

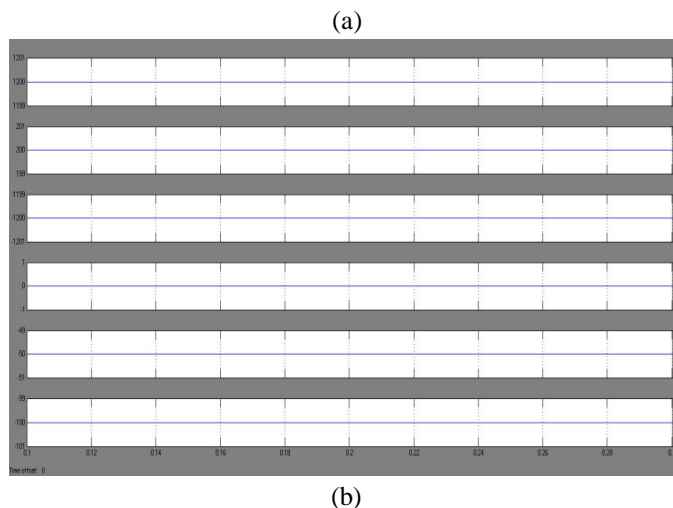
(c) Source current THD at PI



(d) Load current THD with PI

Fig.9. Simulated performance of the proposed DFIG based WECS at fixedwind speed of 10.6 m/sec





(b)
Fig.10.Simulated performance of the proposed DFIG based WECS working as a STATCOM at zero wind speed.

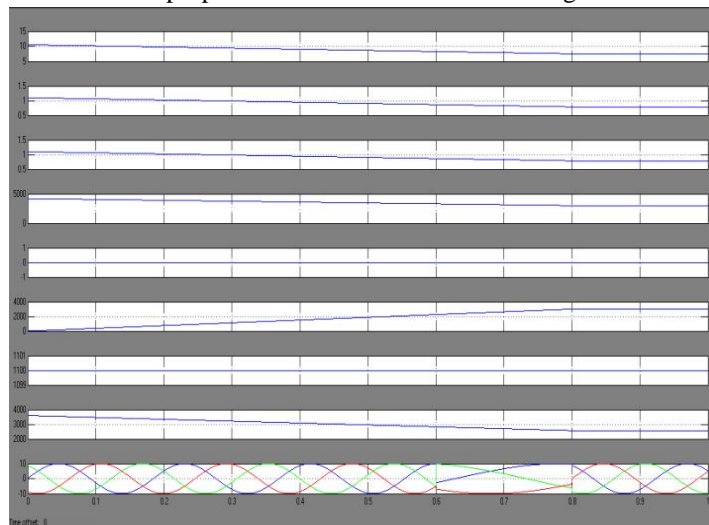


Fig.11. Simulated performance of proposed DFIG for fall in wind speed

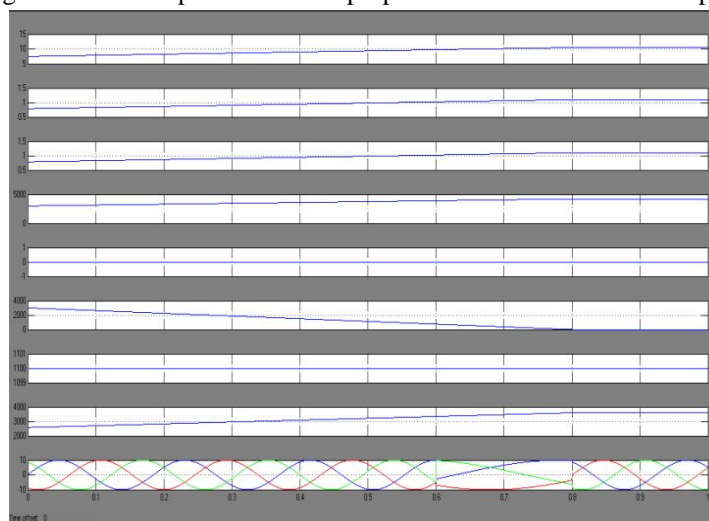


Fig.12. Dynamic performance of DFIG for the rise in wind speed

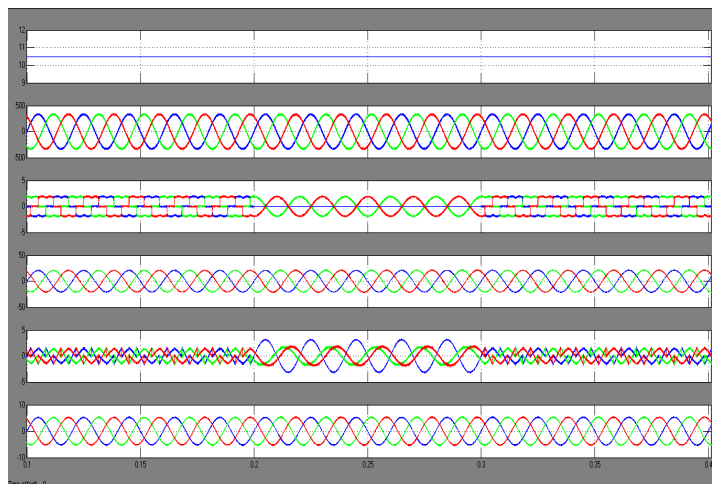


Fig.13. Dynamic performance of DFIG based WECS for the sudden removal and application of local loads.

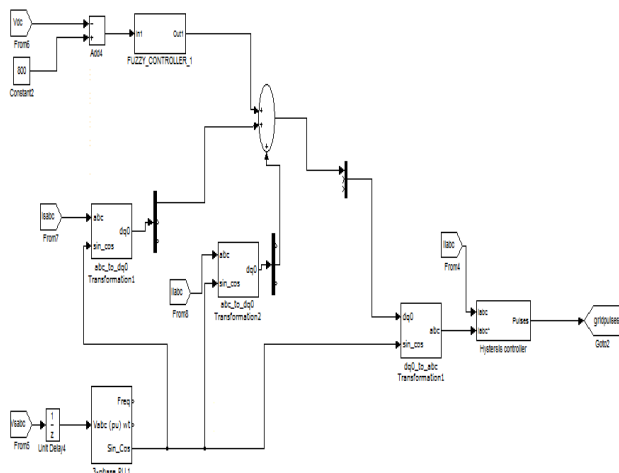


Fig.14. Proposed DFIG based WECS Fuzzy Control circuit

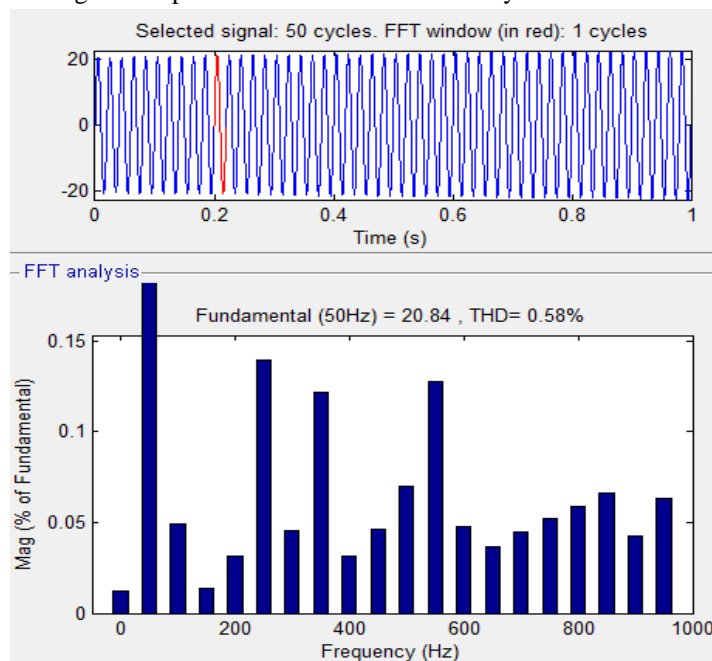


Fig.15. Fuzzy Source current (I_s) THD

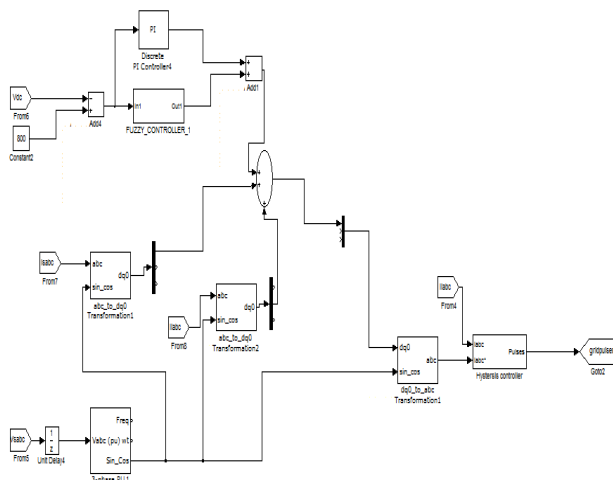


Fig.16. Proposed DFIG based WECS Hybrid Fuzzy control circuit is 0.58%

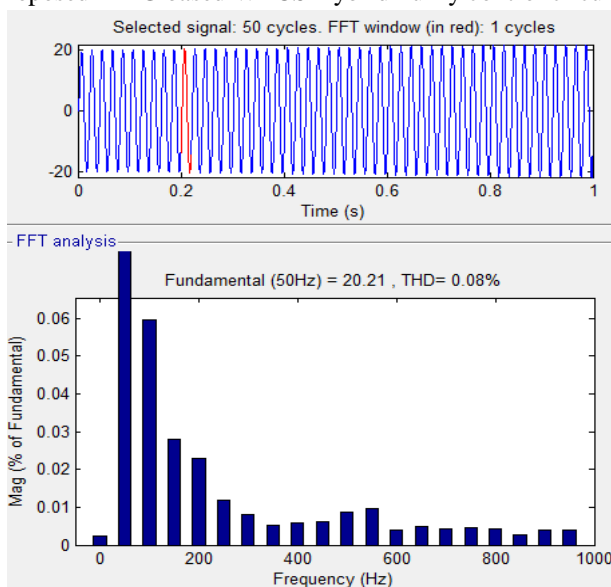


Fig.17. Source current THD with Hybrid fuzzy is 0.08%

VII. CONCLUSION

In this paper the proposed DFIG based WECS has been found capable of supplying regulated power in all wind speeds by introducing BESS in the DC link. The design of BESS in this DFIG based WECS has been presented in detail. The control algorithm of GSC has been modified for feeding regulated power to the grid. The performance of proposed DFIG has been validated through test results for the both fixed and variable wind speeds at all possible rotor speeds. This proposed WECS has been further implemented with PI, fuzzy and hybrid fuzzy controllers for reducing harmonics in power system and improve dynamic response of WECS and the controllers are compared, the simulation results obtained are satisfactorily attained good response.

REFERENCES

- [1] GovadaPanduranga Ganesh, Arjuna Rao A, "Super-Capacitor Energy Storage of DFIG Wind Turbines with Fuzzy Controller," International Journal of Engineering Research and Development, Volume 10, Issue 12 (December 2014), PP.52-66.
- [2] Ganesula Prasad, Shaik Dawood, "A Hybrid AC/DC Micro grid With Fuzzy Logic Controller," International Journal of Engineering Research And Management (IJERM) ISSN : 2349- 2058, Volume-03, Issue-03, March 2016.
- [3] S. S. Murthy, B. Singh, P. K. Goel and S. K. Tiwari, "A Comparative Study of Fixed Speed and Variable Speed Wind Energy Conversion Systems Feeding the Grid", in Proc. IEEE 7th International Conference Power Electronics and Drive Systems, 2007 PEDS '07, 27-30 Nov. 2007, pp.736-743.
- [4] L. Holdsworth, X. G. Wu, J. B. Ekanayake and N. Jenkins, "Comparison of fixed speed and doubly-fed induction wind turbines during power system disturbances," IEE Proc. Generation, Transmission and Distribution, vol. 150, no. 3, pp. 343-352, 13 May 2003.



- [5] M. Mansour, M. N. Mansouri and M. F. Mimouni, "Comparative study of fixed speed and variable speed wind generator with pitch angle control," International Conference on Communications, Computing and Control Applications (CCCA), 3-5 March 2011, pp. 1-7.
- [6] R. Datta and V. T. Ranganathan, "variable-speed wind power generation using doubly fed wound rotor induction machine-a comparison with alternative schemes," IEEE Trans. Energy Con., vol.17, no.3, pp. 414- 421, Sep 2002.
- [7] S. Muller, M. Deicke and R. W. De Doncker, "Doubly fed induction generator systems for wind turbines," IEEE Industry Applications Magazine, vol.8, no.3, pp.26-33, May/Jun 2002.
- [8] Changling Luo, H. Banakar, B. Shen and Boon - Teck Ooi, "Strategies to Smooth Wind Power Fluctuations of Wind Turbine Generator," IEEE Trans. Energy Con., vol.22, no.2, pp.341-349, June 2007.
- [9] H. Polinder, F. F. A. van der Pijl, G. J. de Vilder and P. J. Tavner, "Comparison of direct-drive and geared generator concepts for wind turbines," IEEE Trans. Energy Con., vol. 21, no. 3, pp.725 -733, May 2005.
- [10] C. Abbey and G. Joos, "Super capacitor Energy Storage for Wind Energy Applications," IEEE Transactions on Industry Applications, vol. 43, no. 3, pp. 769-776, May-June 2007.
- [11] J. P. Barton and D. G. Infield, "Energy storage and its use with intermittent renewable energy," IEEE Transactions on Energy Conversion, vol.19, no.2, pp. 441-448, June 2004.
- [12] Liyan Qu and Wei Qiao, "Constant Power Control of DFIG Wind Turbines With Super capacitor Energy Storage," IEEE Transactions on Industry Applications, vol.47, no.1, pp. 359-367, Jan.-Feb. 2011.
- [13] Youngil Kim and R. Harrington, "Analysis of various energy storage systems for variable speed wind turbines," 2015 IEEE Conference on Technologies for Sustainability (SusTech), Ogden, UT, 2015, pp. 7-14.



10.22214/IJRASET



45.98



IMPACT FACTOR:
7.129



IMPACT FACTOR:
7.429



INTERNATIONAL JOURNAL FOR RESEARCH

IN APPLIED SCIENCE & ENGINEERING TECHNOLOGY

Call : 08813907089  (24*7 Support on Whatsapp)